

Proliferation of neutral modes in fractional quantum Hall states

Hiroyuki Inoue, Anna Grivnin, Yuval Ronen, Moty Heiblum, Vladimir Umansky and
Diana Mahalu

Braun Center for Submicron Research, Department of Condensed Matter Physics,
Weizmann Institute of Science, Rehovot 76100, Israel

The fractional quantum Hall effect (FQHE) is a canonical example of a topological phase in a correlated 2D electron gas under strong magnetic field^{1,2}. While electric currents propagate as chiral *downstream* edge modes²⁻⁴, chargeless *upstream* chiral neutral edge modes were recently observed only in *hole-conjugate* states (states filling ν , $n+1/2 < \nu < n+1$, with $n=0,1,2,\dots$), and in the even denominator state $\nu=5/2$ ⁵⁻⁹. It is believed that spontaneous ‘density reconstruction’ near the edges of the 2D gas, leads to multiple counter propagating edge channels, being separated from each other by incompressible strips. Unavoidable disorder induces inter-channel tunneling; accompanied by Coulomb interaction it renormalizes the multiple edge channels to a downstream charge mode and upstream neutral edge mode(s), while maintaining the parity requirements (e.g., the heat conductance along the edge) dictated by the bulk¹⁰⁻¹⁷. Here, we report of highly sensitive shot noise measurements that revealed unexpected presence of neutral modes in a variety of non-hole-conjugate fractional states. As already reported previously⁵, we did not observe neutral modes in any of the integer states. In addition to the upstream neutral edge modes, we were surprised to find also neutral energy modes that propagate through the incompressible bulk. While along the edge, density reconstruction may account for the edge modes, we are not aware of a model that can account for the bulk modes. The proliferation of neutral modes, in every tested fractional state, changes drastically the accepted picture of FQHE states: an insulating bulk and 1D chiral edge channels. The apparent ubiquitous presence of these energy modes may account for decoherence of fractional quasiparticles - preventing observation of coherent interference in the fractional regime.

Charge propagation in the quantum Hall effect regime takes place near the edge of the 2D electron gas in form of *downstream* chiral edge modes (with chirality determined by the direction of the magnetic field); while the bulk is incompressible (gapped) and thus does not contribute to the transport^{1-4,18-19}. In the integer regime, with ν the integer filling factor (being the ratio between the number of electrons to the number of flux quanta, $\phi_0=h/e$), charged excitations are electrons while in the fractional regime (say, $\nu<1$), they are fractionally charged quasiparticles (or quasiholes)²⁰⁻²³. However, as was predicted in the 90's¹⁰⁻¹¹, and recently demonstrated⁵⁻⁹, this picture is, in general, too simple. For, the so called, hole-conjugate states of the FQHE regime, edge *reconstruction* of the electron density is expected to take place at the physical edge of the 2D gas; with counter-propagating electron and hole edge currents. Since such edge currents were never observed¹², tunneling between these edge channels (due to disorder), accompanied by Coulomb interaction, had been proposed to renormalize the ‘multiple current channels’, leading to a *downstream* chiral current mode and *upstream* (counter propagating to the charge modes) neutral (chargeless) mode(s)¹³⁻¹⁵ – as was indeed recently detected in hole-conjugate FQHE states⁵⁻⁹.

Following a significant effort to develop a sensitive heat sensor in a thinly polished substrate²⁴, our group detected the presence of neutral modes in $\nu=2/3, 3/5, 5/3, 8/3$ and $5/2$ via measuring noise, with zero net current, resulting from impinging the modes *upstream* on a partly pinched quantum point contact (QPC) constriction, or, alternatively, by on a non-ideal ohmic contact⁵⁻⁷. The measured noise may result from the fragmentation of the neutral quasiparticles (it is instructive to look at them as electrical dipoles) by a partitioning barrier⁵, or, alternatively, due to local Joule heating of the barrier⁷. Support to the latter mechanism was also provided by observing thermal broadening of conductance peaks^{8,9} or the generation of net thermoelectric current⁹ - both in quantum dots (QDs). Though one can find predictions for edge reconstruction also in integer fillings²⁵ and also in particle-like fractional states²⁶⁻²⁷, they were not observed before. Here, we report on findings of chiral upstream neutral modes, again via sensitive noise measurements, in particle-like fractional states. Moreover, and even more surprising, energy flow through the bulk was

also found in all the tested states. Note, that bulk heat transports in $\nu=1$ ⁸ and in $\nu=4/3$ ²⁸ were recently reported.

Excited neutral modes, carrying energy, can be excited by two possible sources (see schematic illustration in Fig. 1 (also, S1 in Supplementary Section): (i) A partly pinched QPC, which partitions downstream current I_C arriving from S_C ⁷, and (ii) The *hot-spot* at the upstream side of a biased ohmic contact S_N ⁵, fed by current I_N . In the following experiments, neutral modes were converted to downstream current fluctuations, i^2 , with zero net current, in standard ohmic contacts⁷. Voltage fluctuations, $v^2=i^2/\nu^2G_0^2$ (independent of the QPC transmission)²⁹, were amplified by a cryogenic preamplifier; placed along the downstream edge at A_{CE} , along the upstream edge at A_{NE} , or connected to the bulk at A_{NB} . The presence of neutral modes was verified by measuring shot noise in two configurations (Fig. 1): (i) Partitioning I_C by a QPC and measuring the resultant upstream noise at A_{NE} and the bulk noise at A_{NB} - named C→N; and (ii) As in (i), but the noise at A_{CE} was measured in the presence of a neutral mode arriving upstream from S_N - named C+N. The latter measurements allowed measuring the charge of the partitioned quasiparticles and their temperature^{29,30} in presence of an impinging neutral mode. It is worth reminding the reader of the ‘standard’ expression of excess noise (shot noise above the thermal contribution), due to stochastic partitioning (transmission t) of a noiseless beam of charge e^* quasiparticles, $S_i = 2e^* I t(1-t)(\coth x - x^{-1})$, with $x = e^* I \nu^{-1} G_0^{-1} / 2k_B T$, where S_i is the ‘zero frequency’ noise spectral density, k_B the Boltzmann constant, and I the impinging current^{29,30}.

We start with filling $\nu=2/3$ of the first spin-split Landau level, where the presence of upstream neutral modes had been already established^{5,7-9}. We fabricated a device with short propagation distance of the neutral modes, $3.5\mu\text{m}$ & $7\mu\text{m}$, in order to enhance the measured shot noise. At the center of the $\nu=2/3$ conductance plateau, $B=6.7\text{T}$, with the state fully polarized, the neutral mode was measured in the C→N configuration, with $-4\text{nA} \leq I_C \leq 4\text{nA}$ (see Fig. 1). Another configuration, named N→N, relied on exciting the neutral mode by the ‘hot spot’ at the upstream side of S_N by driving current I_N . The neutral mode was partly transmitted by the upstream QPC and generated currentless noise at A_{NE}

(S2 at the Supplementary Section). In all the measurements, only a negligible amount of net current ($<0.5\text{pA}$, via through the bulk) was detected at A_{NE} & A_{NB} ; assuring a negligible contribution to the noise (if carrying poissonian noise (see also Fig. 6b), one would expect $S_I=2eI_{bulk}\sim 3\times 10^{-31}\text{A}^2/\text{Hz}$). A monotonically increasing (currentless) excess noise with I_C was measured upstream along the edge (at A_{NE}) and directly through the bulk (at A_{NB}); both exhibiting $\sim t(1-t)$ dependence (see Figs. 2a & 2b). Two main observations are apparent from the data: (i) The excess noise along the edge in A_{NE} , exhibiting a slight negative curvature, is some ten times higher than that in A_{NB} ; (ii) The excess noise through the bulk in A_{NB} exhibits a slight positive curvature. Note that the integrity of the state is maintained by keeping the excitation voltage in S_C ($150\mu\text{V}$) substantially lower than the presumed energy gap of $\nu=2/3$ ($\sim 780\mu\text{V}$)³¹.

In the C+N configuration at filling $\nu=2/3$, we measured the noise at A_{CE} in the range $4\text{nA}\leq I_C\leq 4\text{nA}$ and $0\text{nA}\leq I_N\leq 4\text{nA}$ (Fig. 3). Two contributions to the downstream excess noise at A_{CE} were measured (Fig. 3a): one due to partitioning of I_C in the presence of I_N , and the other due to fragmentation of the neutral mode arriving from S_N (or excess heating). Assuming these are uncorrelated contributions, we can easily extract the temperature and charge of the partitioned quasiparticles (note, that detailed mechanism of neutral-charge interaction in the QPC is not known)⁵⁻⁷. At $I_N=0$, with increasing I_C the excess noise behaves binomial (above expression), with the partitioned quasiparticle charge $e^*\sim 2e/3$ at temperature $T=25\text{mK}$ (Fig. 3b). As I_N increased from 0 to 4nA , the contribution of the neutral mode to the noise increased, and the partitioned quasiparticle charge gradually decreased from $e^*\sim 2e/3$ to $e^*\sim 0.4e$. Similarly, the temperature of the partitioned quasiparticles increased to $\sim 140\text{mK}$ at $I_N=4\text{nA}$, as shown in Fig. 3c; agreeing qualitatively with previous measurements^{5,32}. We note that such temperature increase barely influenced the transmission t of the QPC.

We move now to $\nu=1/3$, where neutral modes were not observed before; and while not-forbidden theoretically, their presence was not expected. Employing first the C \rightarrow N configuration, with the magnetic field tuned to the center of the conductance plateau, $B=13.5\text{T}$. As shown in Figs. 2c & 2d, excess upstream noise was observed, accompanied

also by noise in A_{NB} . Though considerably weaker than in $\nu=2/3$, the excess noise was easily detected (due to the shorter propagation length and the extremely ‘quiet’ preamplifiers), exhibiting also $\sim t(1-t)$ dependence; with the noise along the edge some eight time stronger than that through the bulk. As in the $\nu=2/3$ case, the excitation voltage is maintained much smaller than the gap energy³¹.

Measurements at the C+N configuration followed at $\nu=1/3$ (Figs. 4). The excess noise followed the familiar dependence on current; however, the partitioned quasiparticle charge varied with bias (even though t was constant). Concentrating on the small bias regime ($I_C < 2\text{nA}$), the partitioned quasiparticle charge (at $I_N=0$) was $e^* \sim 0.78e$ (Fig. 4b). This is not surprising, as quasiparticles bunching is often found when t is not nearly unity³³. As I_N increased, the quasiparticle charge decreased to $e^* = 0.56e$, accompanied by temperature increase of the partitioned quasiparticles to $\sim 85\text{mK}$ (Fig. 4c).

Having established the presence of currentless neutral modes in $\nu=2/3$ and also in the unexpected $\nu=1/3$ states, we also tested other particle-like states, such as $\nu=2/5$ and $\nu=4/3$. In both cases, only the current carried by the inner channels ($2/5-1/3$, and $4/3-1$) was partitioned by the QPC in the C \rightarrow N configuration. The results are qualitatively similar to those in $\nu=1/3$ states. (see S3 in Supplementary Section for C \rightarrow N configuration at $\nu=2/5$). Though it cannot be fully discounted²⁵, integer fillings did not have any measurable noise in the C \rightarrow N configuration; even with $I_C=4\text{nA}$ and background noise level $< 5 \times 10^{-31} \text{A}^2/\text{Hz}$ (see S4 in Supplementary Section).

Since spurious thermal effects may contribute to the excess noise, measurements in the C \rightarrow N configuration were repeated at temperature $T=50, 100, \text{ and } 180\text{mK}$ at $\nu=2/3$ and $\nu=1/3$. Strong reduction of the excess noise at A_{NE} and A_{NB} was observed (Fig. 5). Such noise suppression indicates: (i) The minute bulk current, which increased slightly with temperature (since R_{xx} increased), does not contribute to the excess noise; (ii) The decay of the excess noise with temperature conforms qualitatively with the expected shortening of the decay length with temperature^{13,14}; and (iii) The bulk mode seems to decay much faster

in comparison with the edge mode. Having both similar propagation lengths, it may suggest that the modes are of two different natures.

In order to verify further the presence of upstream neutral modes in particle-like states, we employed a different geometry, which allowed continuously tuning of the filling fraction in the bulk via top gates; albeit not separating the bulk and edge contributions (see Fig. 6a for the schematics). We employed the C→N configuration ($I_C=2.5\text{nA}$); however, instead of partitioning the edge channel with a QPC as above, it was partitioned at the interface between two filling factors: arriving from $\nu_L=1$ region and partitioned into a variable $\nu_R<1$ region – with an assumed ‘hot spot’ at the partitioned region (see Fig. 6a). The length of the interface between TGL and TGR was $3\mu\text{m}$ and the total path length to the amplifier contact was $8\mu\text{m}$. The upstream neutral mode was expected to propagate in the $\nu_R<1$ region, with noise produced in ohmic contact A_{NE} . In Fig. 6b we plotted the measured noise at $B=7\text{T}$ as function of the gate voltage on the right top gate V_{TGR} as well as the undesirable bulk current I_{bulk} and its presumed Poissonian noise $2eI_{bulk}$. Evidence of upstream noise is clear in all fractional fillings between $\nu=2/3$ and $\nu=1/3$. Note that while the bulk current goes up in the compressible regions, the noise goes down – as was described above. As before, the noise in particle-like states is considerably smaller than in $\nu=2/3$ with vanishing bulk current in both cases. Varying the density of the bulk and adjusting correspondingly the magnetic field, we also performed noise measurements at constant filling fractions, with the results shown in some details in the Supplementary Section (S5).

The discovery of such proliferation of neutral energy modes, changes the accepted view of current and energy transport by chiral edge channels and the bulk in the FQHE. Though only a few fractional states had been tested here, it is highly likely that most fractional states, being particle-like or hole-conjugate-like, harbor a much more complex edge structures. Moreover, the bulk, being incompressible, seems to be active energetically. Since the topological properties of the bulk dictate a conserved quantum thermal conductance for each state (*e.g.*, zero for $\nu=2/3$; one for $\nu=1/3$)¹⁵, it imposes fundamental differences between particle-like and hole-like states. Even for a sharp confinement potential (compared to magnetic length), the $\nu=2/3$ state must consist of two oppositely

propagating channels, while the $\nu=1/3$ must not to reconstruct. Moreover, rather than having only two oppositely propagating edge channels in the $\nu=2/3$ state, for a shallow enough confining potential, an additional puddle of $\nu=1/3$ state can nucleate on the edge (thus adding a pair of counter-propagating $1/3$ channels)^{34,35}. In fact, our measurements were performed with ‘gate defined’ 2D structures (see Fig. 1), and thus, the electron density decreased gradually towards the edge – encouraging such edge reconstruction. Hence, such edge reconstruction might be eliminated in the latter, by sharpening the profile of the density near the edge, and thus affecting the presence and the nature of the neutral modes.

How can one envision the likely edge reconstruction in $\nu=1/3$ state? Very much like the parameters that play role in the $\nu=2/3$ state, a competition among the confinement potential, magnetic length, and the Coulomb interaction, dictate the electron distribution near the edge^{34,35}. The electron density should, at first, decrease monotonously towards the edge, leading to a downstream channel. Subsequently, two (at least) counter-propagating channels must emerge: one upstream due to an increased electron density, and one downstream due to the density dropping to zero at the depletion region near the edge. Yet, the net conductance must be $G_0/3$; necessitating an upstream neutral mode. It is unlikely that the two added channels should be of $\nu=1/3$ character; since the original $1/3$ channel and the added upstream one will easily localize due to disorder³⁶. Hence, the added two channels may be of lower filling, such as $\nu=1/5$, or, alternatively, a higher one, such as $\nu=1$. This type of reconstruction may depend on details and should be confirmed experimentally at each fractional filling.

The presence of bulk modes may indicate bulk-edge coupling, even though some of the features and temperature dependence are different²⁸. We are not aware of any prediction of such bulk energy transport, specifically in the fractional regime, which may account for our observation. The immeasurably small noise in A_{NB} in the integer regime likely eliminates energy transport via crystal phonons emerging from the region of potential imbalance (ohmic contact or QPC)²⁸.

The proliferation of energy modes, especially those excited by partitioning of current in a QPC, may explain the difficulty in observing interference of fractional charges in interferometers that are based on charge partitioning. Drawing energy from the charged quasiparticles in the partitioning process, the modes may serve as sources of decoherence – preventing studying the statistics of fractionally charged quasiparticles.

METHODS SUMMARY

For the noise measurement, a voltage source with $1\text{G}\Omega$ resistor at its output fed the DC currents and the generated noise signals at amplifier contacts, filtered with an LC circuit tuned to ~ 800 kHz, were amplified first by a cooled, home-made, preamplifier with voltage gain 11 and subsequently by a room temperature amplifier (NF-220F5) with voltage gain 200. The amplified signal was measured by a spectrum analyzer with the bandwidth of 10 kHz. In order to monitor the net current reaching the amplifiers A_{NE} and A_{NB} , $5\mu\text{V}_{\text{RMS}}$ at the resonant frequency on top of the DC currents was applied from the sources and measured at amplifiers with the bandwidth of 30Hz. For the differential conductance measurement to characterize the QPC, we sent $0.5\mu\text{V}_{\text{RMS}}$ at the resonant frequency along with DC currents and measured at A_{CE} with the bandwidth of 30Hz.

Acknowledgements

We thank Y. Gefen and Y. Meir for useful discussions. We acknowledge the partial support of the Israeli Science Foundation (ISF), the Minerva foundation, the U.S.-Israel Bi-National Science Foundation (BSF), the European Research Council under the European Community's Seventh Framework Program (FP7/2007-2013)/ERC Grant agreement No. 227716, and the German Israeli Project Cooperation (DIP).

Figures

Figure 1. | Schematics of the experiment. The device was fabricated on a GaAs/AlGaAs heterostructure, with 2DEG embedded 130nm below the surface whose carrier density is $1.0 \times 10^{11} \text{cm}^{-2}$ and the dark mobility is $5.1 \times 10^6 \text{cm}^2/\text{Vs}$ at 4.2K. The light blue colored region is the mesa embedding the 2DEG. The yellow pads are standard NiAuGe ohmic contacts, grounds (G), amplifiers (A_{CE} , A_{NE} & A_{NB}), and sources, S_C and S_N , driving charge current I_C (blue thick arrows) and neutral current I_N (red thick arrow). The grounded contacts were tied directly to the cold finger of the dilution refrigerator. Heating the mixing chamber raised the temperature of the electrons. The QPC (green lines) was formed by negatively biased split-gates (10nm Ti/30nm Au) with a 660nm wide opening, controlling the transmission probability t . The distance between S_N and the QPC was $3.5 \mu\text{m}$. Each amplifier contact was followed by a resonant circuit (peaking $\sim 800 \text{kHz}$) and a cryogenic voltage amplifier. A_{NE} sits at $7 \mu\text{m}$ along the edge upstream from the QPC, measuring the upstream neutral edge mode solely. A_{NB} is located at $8.5 \mu\text{m}$ over the mesa from the QPC, measuring the bulk mode solely. A_{CE} was to measure the noise in the downstream charge mode. Thin arrows are unbiased channels. We employed two configurations: (i) C \rightarrow N, driving only I_C , partitioned at the QPC and exciting the neutral modes if they were to exist, and detecting their presence by measuring the noise at A_{NE} and A_{NB} simultaneously and (ii) C+N, driving both I_C and I_N and measuring the noise at A_{CE} . The presence of the neutral modes can modify the effective charge and temperature of tunneling quasiparticles.

Figure 2. | C \rightarrow N noise at $\nu=2/3$ and $1/3$ for several QPC transmissions. The configuration C \rightarrow N allows us to detect the neutral modes in the upstream edge and over the bulk separately. **a**, In $\nu=2/3$, the C \rightarrow N noise at A_{NE} for $-4 \text{nA} \leq I_C \leq 4 \text{nA}$ with transmissions $t=0.65, 0.90$ and 1.00 . As $|I_C|$ increases, the noise also increases monotonically. The magnitude of the noise approximately go as $t(1-t)$. **b**, In $\nu=2/3$, the C \rightarrow N noise at A_{NB} measured simultaneously with A_{NE} . The magnitude of the noise in A_{NB} is about ten times smaller than that in A_{NE} . **c**, In $\nu=1/3$, the C \rightarrow N noise at A_{NE} for $-4 \text{nA} \leq I_C \leq 4 \text{nA}$ with transmissions $t = 0.64, 0.72$ and 1.00 . The noise again increases

monotonically with $|I_C|$. The magnitude of the noise follows nearly $t(1-t)$. **d**, In $\nu=1/3$, the C \rightarrow N noise at A_{NB} measured simultaneously with A_{NE} . The magnitude of the noise in A_{NB} is about 7 times weaker than that in A_{NE} . No kink that may originate from the bulk gap was seen in any cases above.

Figure 3. | C+N noise at $\nu=2/3$. The influence of the I_N on the partitioning the charge current I_C also provides indications of the presence of the neutral modes. **a**, The C+N noise at A_{CE} for $-4\text{nA} \leq I_C \leq 4\text{nA}$ with $t=0.72$ was measured in the presence of $0\text{nA} \leq I_N \leq 4\text{nA}$ in steps of 0.5nA . While the traces are merging at high I_C region, one can clearly see an increase in the cut at $I_C=0\text{nA}$, which is consistent with the C \rightarrow N measurement and shows the N \rightarrow C process is also present. Note that the transmission as a function of I_C was barely affected by the presence of I_N . **b**, The fitted temperature as a function of I_N shows the rise of the electron temperature, from about 20mK up to 140mK , with increasing I_N . **c**, The extracted effective charge as a function of I_N shows the suppression of the effective charge, approximately from $2e/3$ down to $e/3$, as reported before.

Figure 4. | C+N noise at $\nu=1/3$. Another verification of the neutral mode in $\nu=1/3$ in the C+N configuration. **a**, The C+N noise at A_{CE} for $-4\text{nA} \leq I_C \leq 4\text{nA}$ with $t=0.83$ was tested with $0\text{nA} \leq I_N \leq 4\text{nA}$ in steps of 1nA . A distinct increase in the low $|I_C|$ region ($\leq 2\text{nA}$) showed up, again being consistent with the C \rightarrow N measurement and witnessing the N \rightarrow C process. Note that I_N had negligible effect on the transmission as a function of I_C . **b**, The electron temperature as a function of I_N rose from about 25mK up to 80mK with increasing I_N . **c**, The effective charge as a function of I_N decayed approximately from $0.8e$ down to $0.5e$, relaxing the quasiparticles bunching, similar to a previous study.

Figure 5. | C \rightarrow N noise at $\nu=2/3$ and $1/3$ at elevated temperatures. We repeated the measurement of the C \rightarrow N noise at $50, 100$ and 180mK for $\nu=2/3$ and $1/3$ at both amplifiers. In all the cases, the noise decayed with raising the temperature. The bulk noise weakened

faster than the edge noise, indicating that the two noises were mediated by different modes. **a**, In $\nu=2/3$, the $C \rightarrow N$ noise measured at A_{NE} for $-4\text{nA} \leq I_C \leq 4\text{nA}$ with $t = 0.65$. **b**, In $\nu=2/3$, the $C \rightarrow N$ noise measured at A_{NB} simultaneously with A_{NE} . **c**, In $\nu=1/3$, the $C \rightarrow N$ noise measured at A_{NE} for $-4\text{nA} \leq I_C \leq 4\text{nA}$ with transmissions $t = 0.64$. **d**, In $\nu=1/3$, the $C \rightarrow N$ noise measured at A_{NB} simultaneously with A_{NE} .

Figure 6. | Additional test of neutral modes in a top-gated device. We also investigated the presence of the neutral modes with a density-tunable device but without any QPC in the $C \rightarrow N$ configuration. **a**, The 2DEG was embedded within the light-blue line and the yellow pads are ohmic contacts (the source S_C and the amplifier A_{NE} to measure the $C \rightarrow N$ noise and ground G). Note that this configuration does not measure the edge contribution and the bulk contribution separately. The blue (red) arrows depict the charge (neutral) current. Top gates, colored in light green, for the left (TGL) and right halves (TGR) of the mesa tuned the local filling factors ν_L and ν_R , respectively. We varied ν_R by the gate voltage V_{TGR} on TGR and adjusted ν_L to be at 1 throughout the experiment. The defining gate (DG) in dark-green fully depleted the 2DEG underneath always. The density of 2DEG at $V_{TGR}=0\text{V}$ was $1.3 \times 10^{11} \text{cm}^{-2}$. The interface of the left and right top gates was $3\mu\text{m}$ and the path length between the interface and the amplifier contact was $8\mu\text{m}$. **b**, At $B=7\text{T}$, driving $I_C=2.5\text{nA}$, the $C \rightarrow N$ noise as a function of V_{TGR} was measured (blue dots) simultaneously with the bulk current I_{bulk} (the Poissonian noise $2eI_{bulk}$ in red dots). The filling fractions ($\nu_R=1/3, 2/5, 3/5, 2/3$ and 1) were specified along the plot. The noise stayed finite at all the fillings except for $\nu_R=1$ and but gradually went down towards $\nu_R=1/3$, which is compatible with the observations shown above. Particularly, it is notable that, upon approaching $\nu_R=1/3$ after $\nu_R=2/5$, the bulk current vanished while the noise increased.

References

1. Das Sarma, S. & Pinczuk, A. *Perspective in Quantum Hall Effects: Novel Quantum Liquid in Low-Dimensional Semiconductor Structures* (Wiley, 1997).
2. Wen, X. G. Topological orders and edge excitations in FQH states, *Adv. Phys.* **44**, 405 (1995).
3. Halperin, B. I. Quantized Hall conductance, current-carrying edge states, and the existence of extended states in a two-dimensional disordered potential. *Phys. Rev. B* **25**, 2185–2190 (1982).
4. Wen, X. G. Chiral Luttinger liquid and the edge excitations in the fractional quantum Hall states. *Phys. Rev. B* **41**, 12838–12844 (1990).
5. Bid, A., Ofek, N., Inoue, H., Heiblum, M., Kane, C. L., Umansky, V. & Mahalu, D. Observation of neutral modes in the quantum Hall regime. *Nature* **466**, 585 - 590 (2010).
6. Dolev, M., Gross, Y., Sabo, R., Gurman, I., Heiblum, M., Umansky, V. & Mahalu, D. Characterizing Neutral Modes of Fractional States in the Second Landau Level. *Phys. Rev. Lett.* **107**, 036805 (2011).
7. Gross, Y., Dolev, Heiblum, M., Umansky, V. & Mahalu, D. Upstream Neutral Modes in the Fractional Quantum Hall Effect Regime: Heat Waves or Coherent Dipoles. *Phys. Rev. Lett.* **108**, 226801 (2012).
8. Venkatachalam, V., Hart, S., Pfeiffer, L., West, K. & Yacoby, A. Local thermometry of neutral modes on the quantum Hall edge. *Nature Physics* **8**, 676-681 (2012).
9. Gurman, I., Sabo, R., Heiblum, M., Umansky, V. & Mahalu, D. Extracting net current from an upstream neutral mode in the fractional quantum Hall regime. *Nature Comm* **3**, 1289 (2012).
10. MacDonald, A. H. Edge states in fractional quantum Hall effect regime. *Phys. Rev. Lett.* **64**, 220–223 (1990).
11. Johnson, M. D. & MacDonald, A. H. Composite edges in $\nu=2/3$ fractional quantum Hall effect. *Phys. Rev. Lett.* **67**, 2060–2063 (1991).

12. Ashoori, R. C., Stormer, H. L., Pfeiffer, L. N., Baldwin, K. W. & West, K. Edge magnetoplasmons in time domain. *Phys. Rev. B* **45**, 3894–3897 (1992).
13. Kane, C. L., Fisher, M. P. A. & Polchinski, J. Randomness at the edge: theory of quantum Hall transport at filling $\nu=2/3$. *Phys. Rev. Lett.* **72**, 4129 - 4132 (1994).
14. Kane, C. L. & Fisher, M. P. A. Impurity scattering and transport of fractional quantum Hall edge states. *Phys. Rev. B* **51**, 13449 -13466 (1995).
15. Kane, C. L. & Fisher, M. P. A. Quantized thermal transport in the fractional quantum Hall effect. *Phys. Rev. B* **55**, 15832–15837 (1997)
16. Levin, M., Halperin, B. I. & Rosenow, B. Particle-hole symmetry and the Pfaffian state. *Phys. Rev. Lett.* **99**, 236806 (2007).
17. Lee, S.S., Ryu, S., Nayak, C. & Fisher, M. P. A. Particle-hole symmetry at the $\nu=5/2$ quantum Hall state. *Phys. Rev. Lett.* **99**, 236807 (2007).
18. Laughlin, R. B. Anomalous quantum Hall effect: An incompressible quantum fluid with fractionally charged excitations. *Phys. Rev. Lett.* **50**, 1395-1398 (1983).
19. Wen, X. G. Chiral Luttinger liquid and the edge excitations in the fractional quantum Hall states. *Phys. Rev. B* **41**, 12838–12844 (1990).
20. de-Picciotto., R. Reznikov, M., Heiblum, M., Umansky, V., Bunin, G. & Mahalu, D. Direct observation of a fractional charge. *Nature* **389**, 162-164 (1997).
21. Saminadayar, L., Glattli, D. C., Jin, Y. & Etienne, B. Observation of the $e/3$ fractionally charged Laughlin quasiparticle. *Phys. Rev. Lett.* **79**, 2526-2529 (1997).
22. Martin, J., Ilani, S., Verdene, B., Smet, J., Umansky, V., Mahalu, D., Schuh, D., Abstreiter, G. & Yacoby, A. Localization of fractionally charged quasi-particles. *Science* **305**, 980-983 (2004).
23. Ofek, N., Bid, A., Heiblum, M., Stern, A., Umansky, V. & Mahalu, D. The role of interactions in an electronic Fabry-Perot interferometer operating in the quantum Hall regime. *Proc. Natl. Acad. Sci. USA* **107**, 5276.
24. Granger, G., Eisenstein, J. P. & Reno, J. L. Observation of chiral heat transport in the quantum Hall regime. *Phys. Rev. Lett.* **102**, 086803 (2009)
25. Chamon, de C. C. & Wen, X. G. Sharp and smooth boundaries of quantum Hall liquids. *Phys. Rev. B* **53**, 4033–4053 (1993).
26. Brey, L. Edge states of composite fermions. *Phys. Rev. B* **50**, 11861–11871 (1994)

27. Chklovskii, D. B. Structure of fractional edge states: A composite-fermion approach. *Phys. Rev. B* **51**, 9895-9902 (1995)
28. Altimiras, C., Le Sueur, H., Gennser, U., Cavanna, A., Mailly, D. & Pierre, F. Chargeless heat transport in the fractional quantum Hall regime. *Phys. Rev. Lett.* **109**, 026803 (2012).
29. Heiblum, M. Quantum shot noise in edge channels. *Phys. Status Solidi b* **49**, 8227–8241 (2006).
30. Martin, T. & Landauer, R. Wave-packet approach to noise in multichannel mesoscopic systems. *Phys. Rev. B* **45**, 1742-1755 (1992).
31. Du, R. R., Stormer, H. L., Tsui, D. C., Pfeiffer, L. N. & West, K. Experimental evidence for new particles in the fractional quantum Hall effect. *Phys. Rev. Lett.* **70**, 2944-2947 (1993).
32. Bid, A., Ofek, N., Heiblum, M., Umansky, V. & Mahalu, D. Shot noise and charge at the $2/3$ composite fractional quantum Hall state. *Phys. Rev. Lett.* **103**, 236802 (2009).
33. Griffiths, T. G., Comforti, E., Heiblum, M., Umansky, V. & Mahalu, D. Evolution of quasiparticle charge in the fractional quantum Hall regime. *Phys. Rev. Lett.* **85**, 3918 (2000).
34. Meir, Y. Composite Edge states in the $\nu = 2/3$ Fractional quantum hall regime *Phys. Rev. Lett.* **72**, 2624 (1994).
35. Wang, J., Meir, Y. & Gefen, Y. Edge reconstruction in the $\nu = 2/3$ fractional Quantum Hall regime. *arXiv* 1305.6029 (1994).
36. Kane, C. L. & Fisher, M. P. A. Line junctions in the quantum Hall effect. *Phys. Rev. B* **56**, 15231- 15237 (1997).

Figure 1

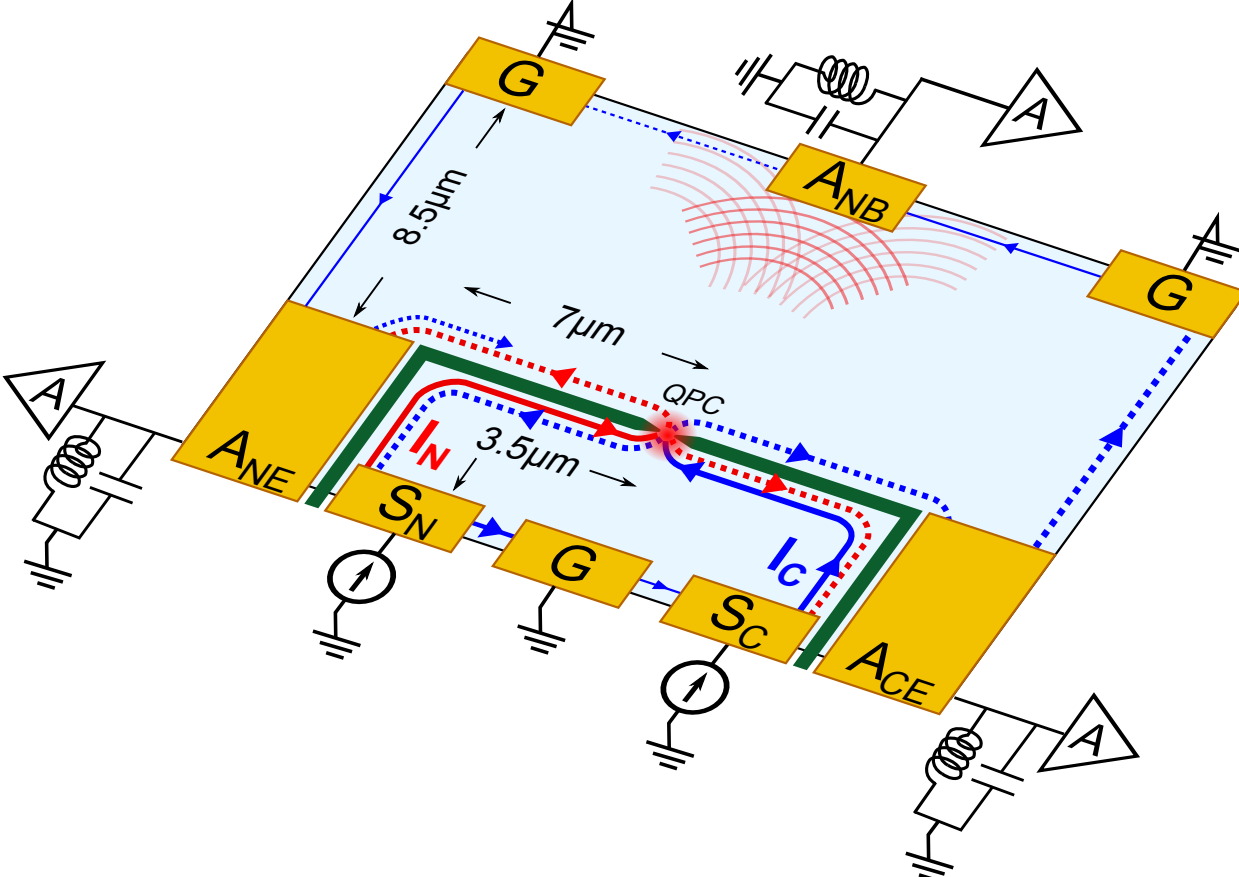


Figure 2

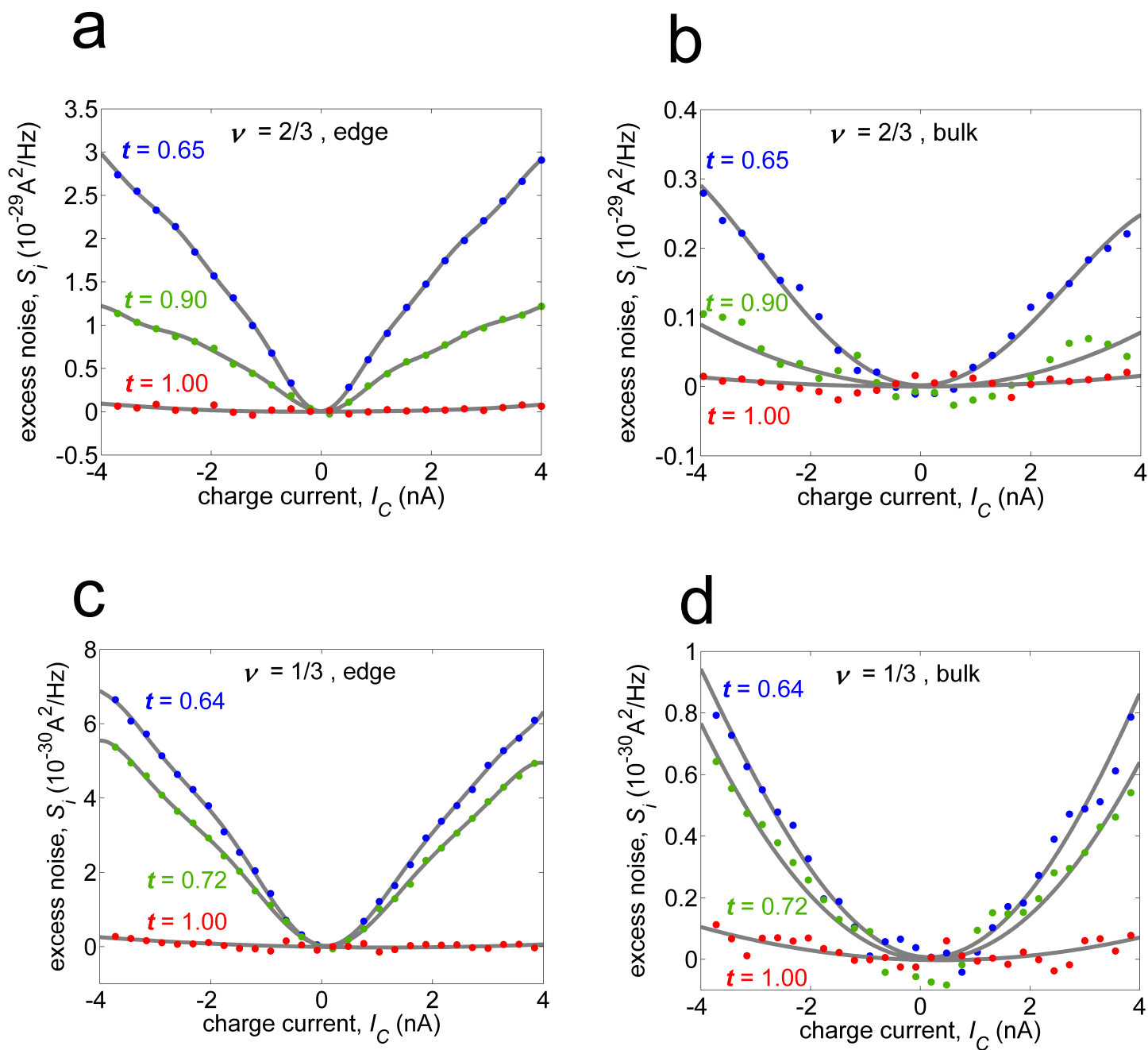


Figure 3

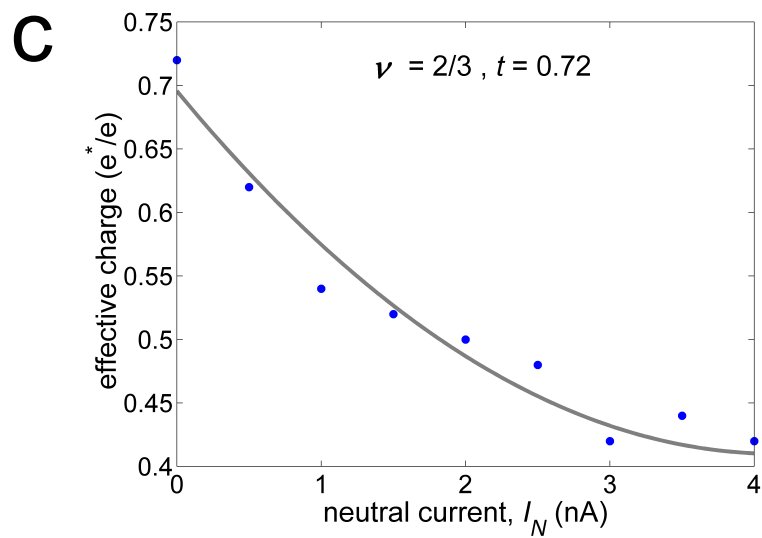
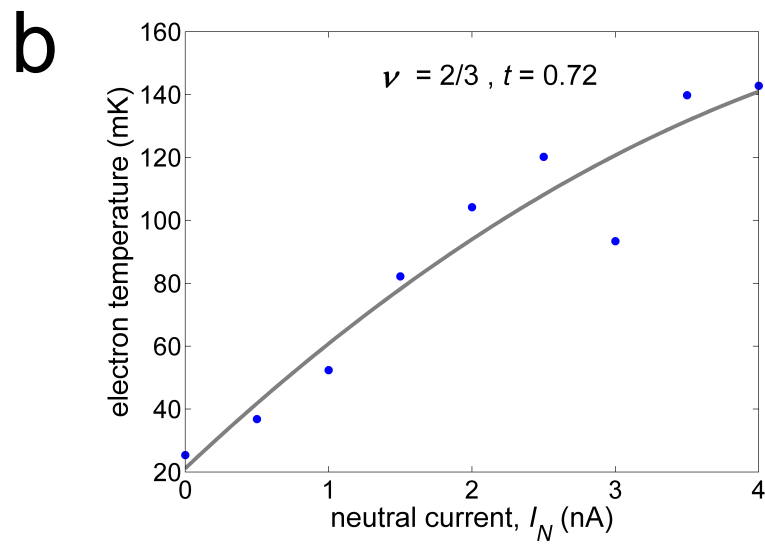
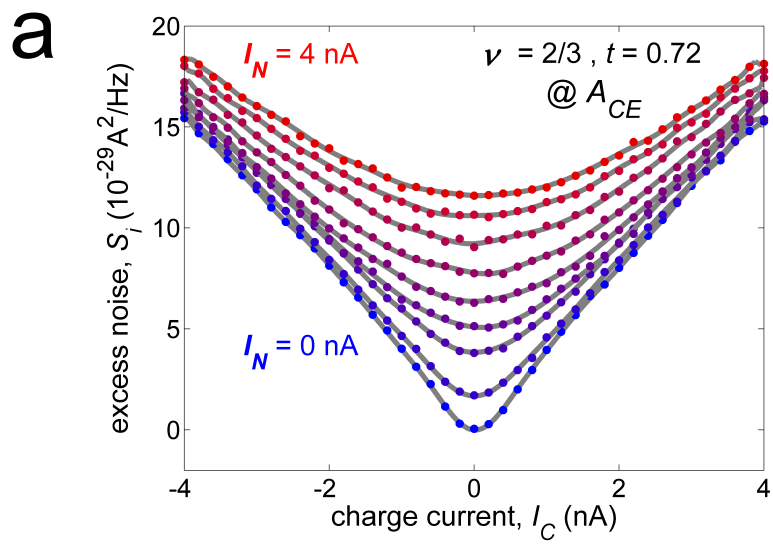


Figure 4

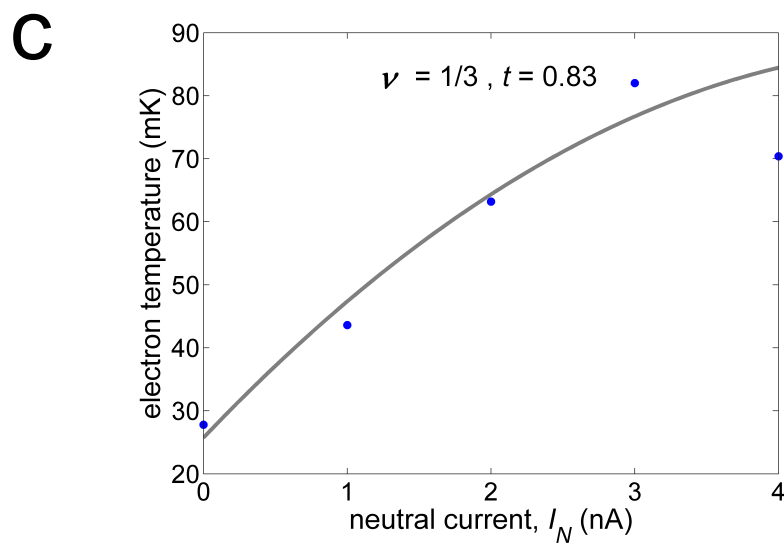
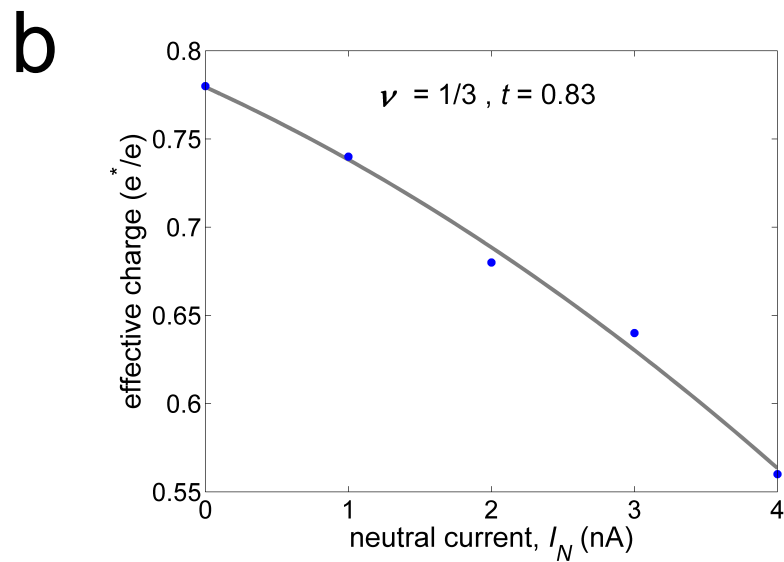
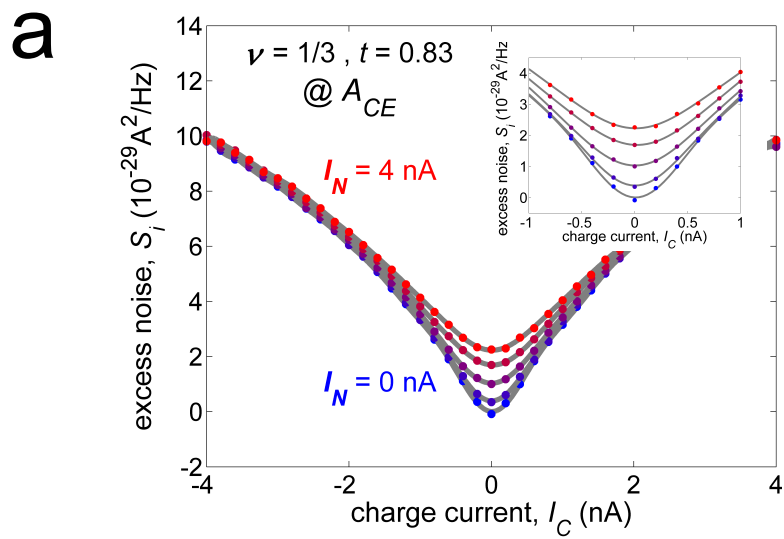
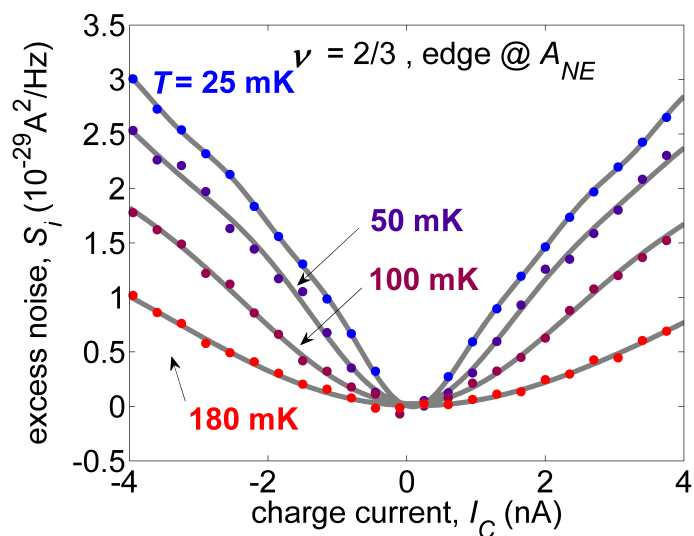
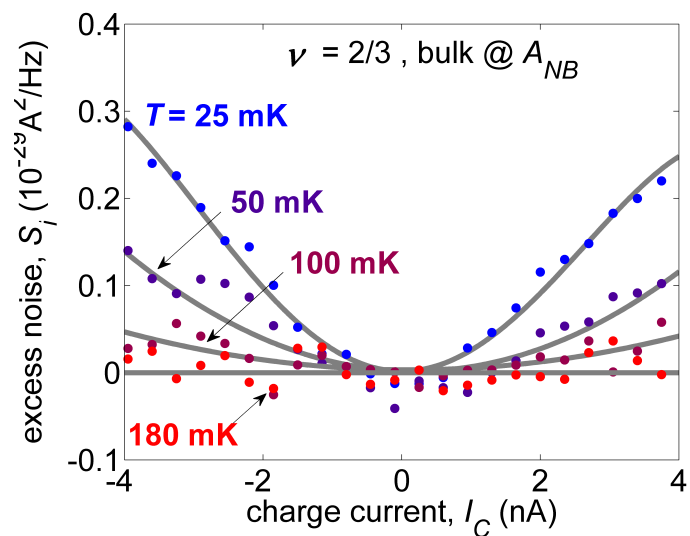


Figure 5

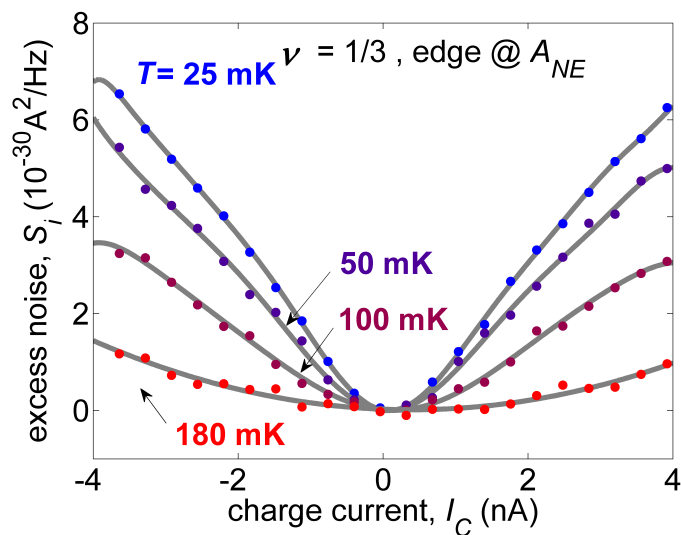
a



b



c



d

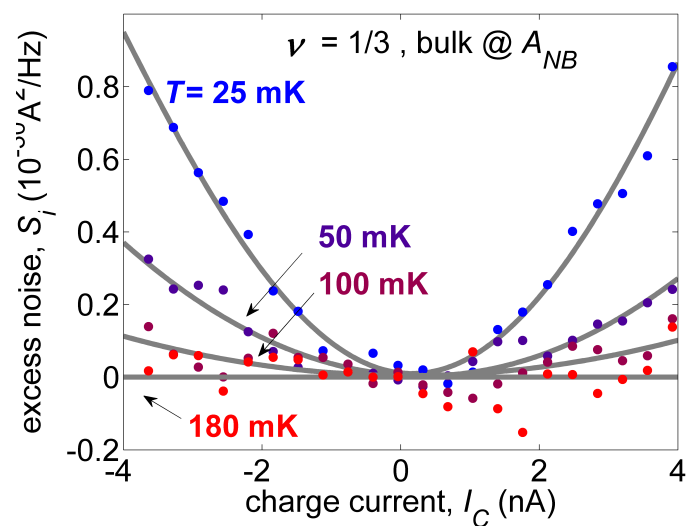
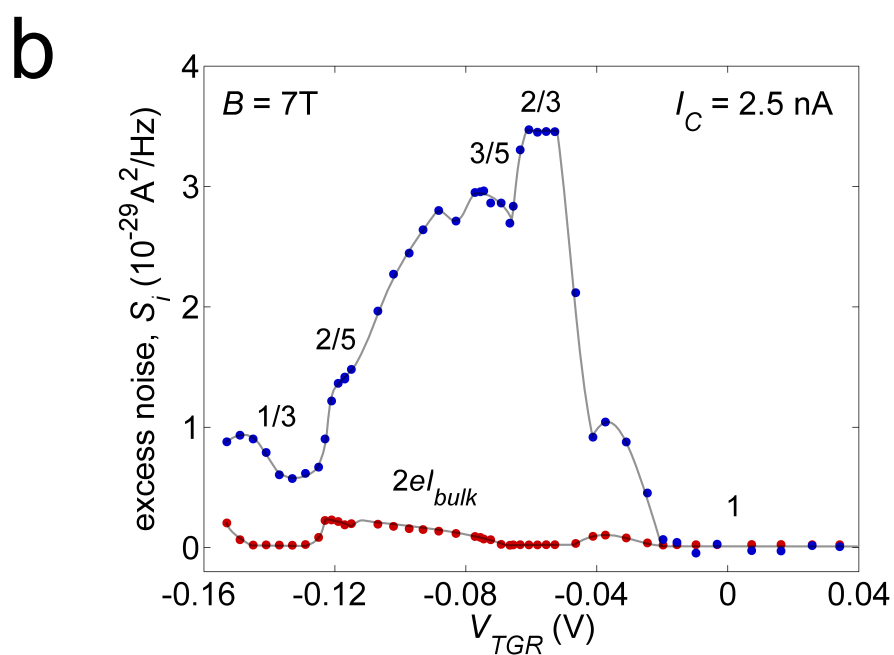
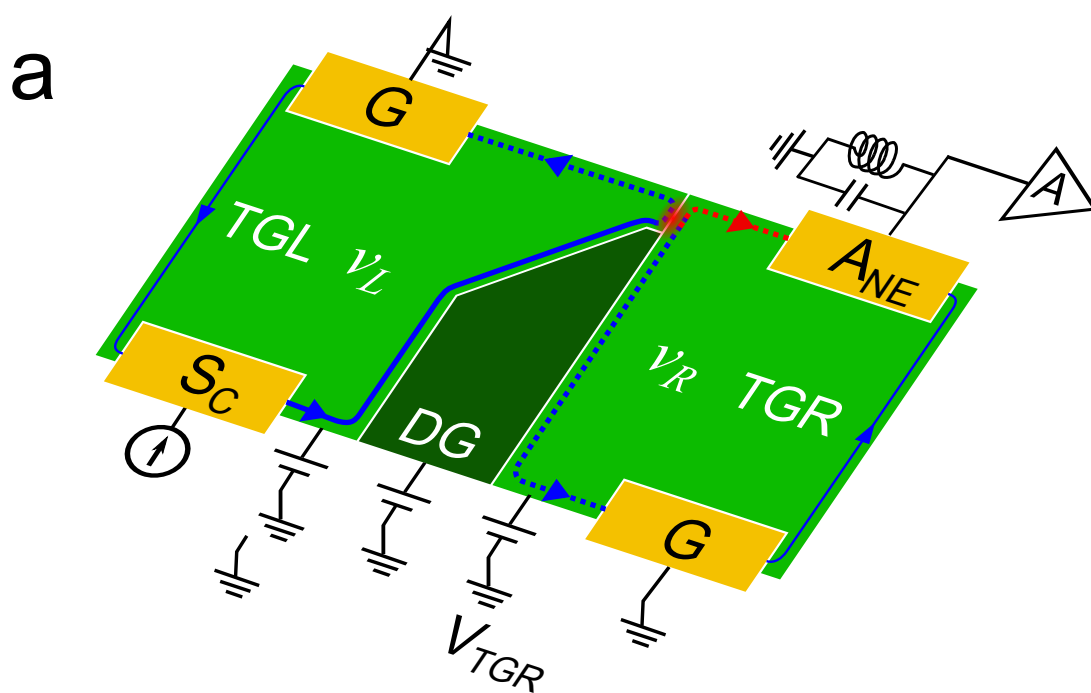


Figure 6



Supplementary Materials

Proliferation of neutral modes in fractional quantum Hall states

Hiroyuki Inoue, Anna Grivnin, Yuval Ronen, Moty Heiblum, Vladimir Umansky and
Diana Mahalu

Braun Center for Submicron Research, Department of Condensed Matter Physics,
Weizmann Institute of Science, Rehovot 76100, Israel

S1. Scanning electron micrograph images of the employed devices

S2. N→N noise at $\nu = 2/3$

S3. C→N noise at $\nu = 2/5$

S4. C→N noise at $\nu = 1$

S5. C→N noise with density-tunable device

S1. Scanning electron micrograph images of the employed devices

In the present experiment, three kinds of configurations on different substrates were employed. The main samples were grown on a GaAs/AlGaAs heterostructure substrate with 2DEG embedded 116nm below the surface whose carrier density is $1.0 \times 10^{11} \text{cm}^{-2}$ and the dark mobility is $5.1 \times 10^6 \text{cm}^2/\text{Vs}$ at 4.2K (substrate 1). Two kinds of designs shown in Fig. S1a and S1b were made on this substrate. All the measurements described in the main manuscript were done on these samples. Let us denote the devices as A1 and B1 respectively (C→N noise measurement on A1 and C+N noise measurement on B1). Another kind of sample with top gates (shown in Fig. S1c) was fabricated on a substrate 2DEG with the carrier density of $1.3 \times 10^{11} \text{cm}^{-2}$ (substrate 2). Let us denote it as device C2. The device C2 was utilized to take the data of Fig. 6. In this supplementary section (S6), another set of data was taken with a device of the design of Fig. S1b grown on a different substrate (substrate 3). Let us denote it as device B3. The substrate embedded 2DEG (113nm below the surface) with the carrier density of $1.2 \times 10^{11} \text{cm}^{-2}$ and the dark mobility $4.2 \times 10^6 \text{cm}^2/\text{Vs}$ at 4.2K.

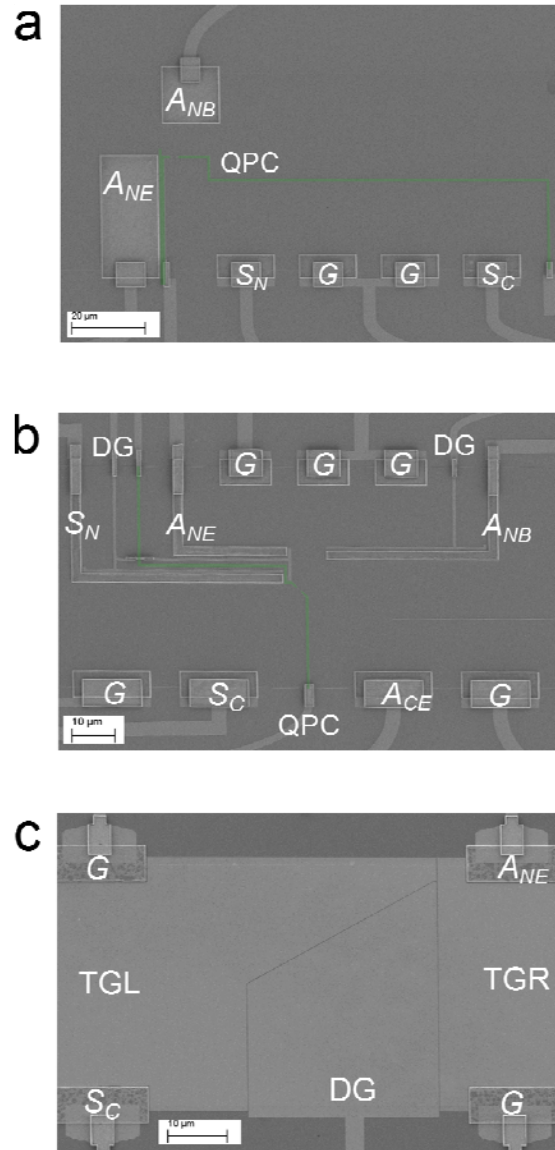


Figure S1. | Scanning electron micrograph images of the employed devices. We employed three kinds of designs from **a** to **c**. The configurations **a** and **b** are equivalent to the schematic illustration depicted in Fig. 1. They differ mainly in the distances between the contact S_N and QPC, which were about $40\mu\text{m}$ in **a** and $3.5\mu\text{m}$ in **b**. For the detailed description of the samples, see the caption of Fig. 1 and Fig. 6a. The green high-lighted strips are the QPCs. The DGs always depleted the electron gas underneath.

S2. N→N noise at $\nu = 2/3$

In the device B3 the N→N noise at $\nu=2/3$ and $B=8.1\text{T}$ was examined as a function of the QPC transmission probability t (0.97, 0.78, 0.65, 0.49, 0) for $-4\text{nA} \leq I_N \leq 4\text{nA}$. Here, the N→N configuration means to source from S_N and to measure at A_{NE} . The measured noise exhibited maximum when $t=0.97$ and monotonously decreased approximately as t down to vanishing small noise.

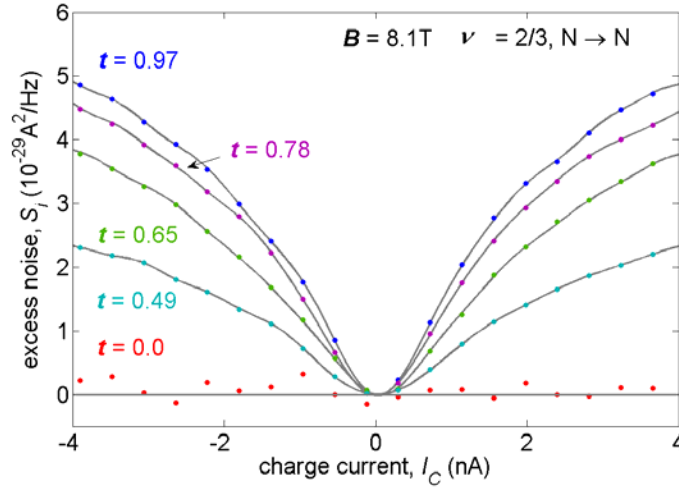


Figure S2. | N→N noise at $\nu = 2/3$. Employing the sample with the density of $1.2 \times 10^{11} \text{cm}^{-2}$, the N→N configuration allows measuring noise of the neutral mode directly, without involving charge partitioning. We sourced current I_C from S_N and measure the noise reaching A_{NE} . Performing the measurements in $\nu=2/3$, for $-4\text{nA} \leq I_C \leq 4\text{nA}$ with QPC transmissions $t=0.97, 0.78, 0.65, 0.49$ and 0.0 . As $|I_C|$ increases the noise also increases monotonically. The amplitude of the noise ascends with the transmission t .

S3. C→N noise at $\nu = 2/5$

In the device B3 the C→N noise at $\nu=2/5$ and $B=11.2\text{T}$ was tested. Here, the edge of $\nu=2/5$ possess two channels corresponding to the inner $2/5$ channel and the outer $1/3$ channel and each carries $I_C/6$ and $5I_C/6$ of the injected current I_C , which corresponds to the conductance of $G_0/15$ and $G_0/3$, respectively. Therefore, the transmission of the QPC as a function of the gate voltage exhibits a plateau corresponding to the full transmission of outer $1/3$ channel. The noise measurement was tested for partitioning the inner $2/5$ channel by 0.5, on the plateau of $1/3$, and partitioning the outer $1/3$ channel by 0.8. The excess noise vs effective current ($I_C/6$ and $5I_C/6$ for the inner and the outer channel respectively) is plotted. Finite noises were observed in all the cases including the case on the plateau which we do not expect to observe finite noise. This may be to do with a possible edge reconstruction therein leading to a partial mixing of two channels.

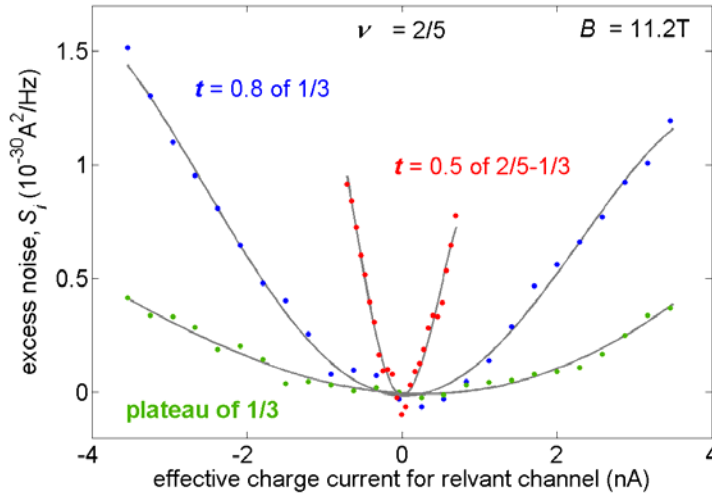


Figure S3. | C→N noise at $\nu = 2/5$. C→N noise at $\nu=2/5$ for several QPC transmissions. In this configuration there are two edge channels propagating one next to the other: An outer channel of $\nu=1/3$ and an inner one with $\nu=2/5$. The noise is measured when either one of the channels is partitioned and when the $1/3$ channel is completely transmitted at the QPC and the $2/5$ is reflected. The C→N noise is plotted as function of the effective current injected into the corresponding channel (The effective current injected into the $1/3$ channel is $5/6 \times I_C$ and the one into the $2/5$ channel is $1/6 \times I_C$).

S4. C→N noise at $\nu = 1$

In both devices A1 and B3, the C→N noise at $\nu=1$ and $B=4.4\text{T}$ and 5.5T were examined with at A_{NE} and A_{NB} for $-4\text{nA} \leq I_C \leq 4\text{nA}$. In all cases, no appreciable noise were seen (all of them stayed below $0.5 \times 10^{-30} \text{ A}^2/\text{Hz}$). However, here we do not exclude the presence of neutral edge modes in integer fillings as reported in a previous study at $\nu=1$ at a higher magnetic field. Since, at lower magnetic fields, it may not be favorable for the integer edges to reconstruct due to rather longer magnetic length being proportional to $B^{-0.5}$. Also, the structure of the edge can depend on details of the sample such as how the edge was defined (wet etch or gate defined), mobility of the 2DEG and etc.

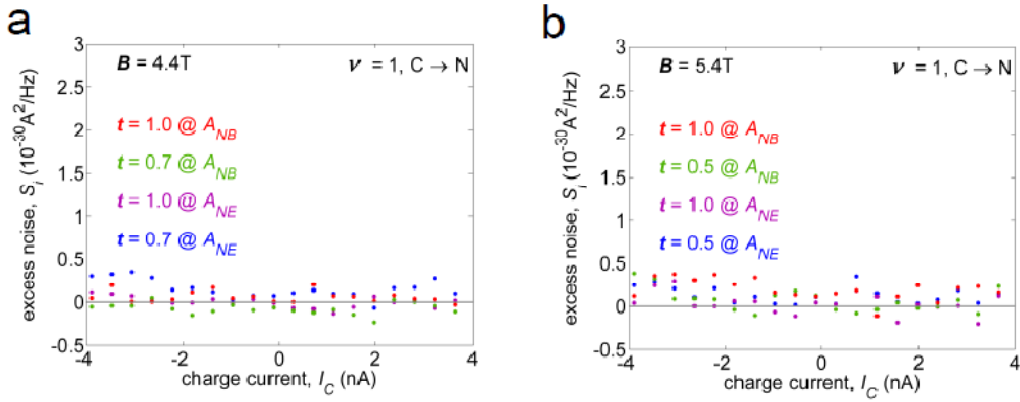


Figure S4. | C→N noise at $\nu = 1$. C→N noise is measured in the upstream edge and over the bulk separately. **a**, In $\nu=1$ (device A1) and $B=4.4\text{T}$ the C→N noise at A_{NB} and at A_{NE} with transmissions $t=1.0, 0.70$ for $-4\text{nA} \leq I_C \leq 4\text{nA}$. Unlike for the fractional fillings, as $|I_C|$ increases, the noise remains below $0.5 \times 10^{-30} \text{ A}^2/\text{Hz}$. **b**, In $\nu=1$ (device B3), $B=5.4\text{T}$ the C→N noise at A_{NB} and at A_{NE} with transmissions $t=1.0, 0.50$ for $-4\text{nA} \leq I_C \leq 4\text{nA}$. Similarly, the noise remains below $0.5 \times 10^{-30} \text{ A}^2/\text{Hz}$.

S5. C→N noise with density-tunable device

With the device C2, the conductance from the left to the right half as a function of V_{TGR} was measured with a standard lock-in technique (at 31Hz). Here, for example, being on the plateau of $\nu_r = 1/3$, a charge current of $I_C/3$ reaches the right half and builds the voltage of $I_C/3 \times 3G_0^{-1} = I_C G_0^{-1}$. Therefore, whenever the diagonal resistance R_{xx} vanishes (forming a Hall plateau), it develops the same voltage of $I_C G_0^{-1}$, which is the unit of the color scale in the Fig. S5a. We repeated such conductance measurement at magnetic fields between 6T and 14T (Fig. S5a). The red strips correspond to the formation of the plateaus $\nu_R=1/3, 2/5, 3/5, 2/3$ and 1 from left to right.

Now, following the $\nu_R=1/3, 2/3$ and 1 strips, the C→N noise was then measured between $B=7T$ and 14T (Fig. S5b). For each filling, the V_{TGR} was adjusted to be on the middle of the plateau. While the noise at $\nu_R=1$ stayed null, the noises in both fillings evolved in a similar fashion and the noise increased as the magnetic field was ramped down. The curves are merely guides for eyes. If we allow ourselves to attribute the observed noise solely to the upstream neutral edge modes because of their dominance over the bulk contribution, a lower density means a stronger disorder due to a weaker screening effect and hence may yield a bigger noise. Since the life time of upstream neutral mode at filling $2/3$ was predicted to be proportional to disorder strength.

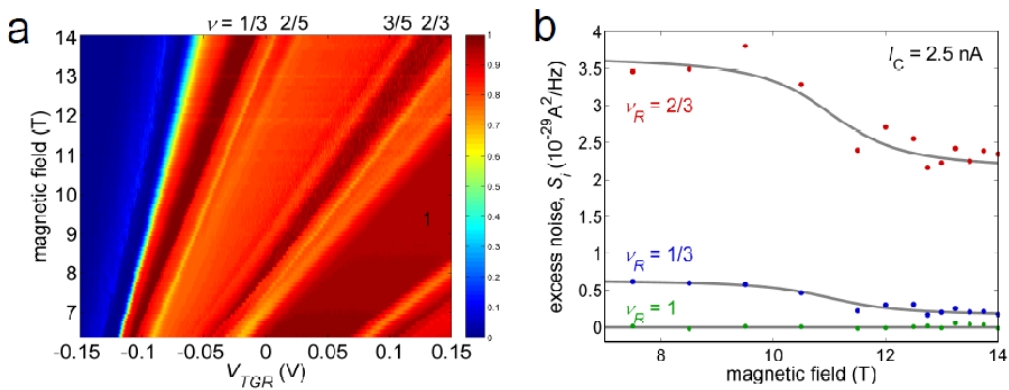


Figure S5. | C→N noise with density-tunable device. **a**, Fan diagram of the right half of the mesa is plotted V_{TGR} vs B . The color scale is in the unit of $I_C G_0^{-1}$ and the red strips correspond to $\nu_R = 1/3, 2/5, 3/5, 2/3$ and 1 from left to right. **b**, The C→N noise for $\nu_R = 1/3, 2/3$ and 1 at various magnetic fields between 7T to 14T was measured. The noise in $\nu_R=1$ stayed zero and the noise in the both fractions increased as the magnetic field was ramped down. The curves are just guide for eyes.